JOURNAL OF SPACECRAFT AND ROCKETS
Vol. 46, No. 3, May–June 2009

Effect of a Rearward-Facing Step on Plasma Ignition in Supersonic Flow

Junya Watanabe,* Naoyuki Abe,* and Kenichi Takita†
Tohoku University, Sendai 980-8579, Japan

DOI: 10.2514/1.39018

The effect of a rearward-facing step on plasma ignition in supersonic flow was experimentally and numerically investigated. In the experiment, the rearward-facing step was installed between a plasma jet torch and a fuel injector. The step height was set at 4 mm and was located 14 mm downstream of the plasma jet torch and 10 mm upstream of the fuel injector. The fuel jet was injected perpendicularly at sonic speed behind the step into the main flow of $M = 1.7$. In the experimental results, with installation of the step, the pseudo shock wave did not travel upstream beyond the step, and there was therefore a threshold electric power input above which a large wall-pressure increase due to combustion appeared. However, the advantage of an installation of the rearward-facing step to the straight duct was not apparently observed in the ignition tests. Numerical simulation showed that the reasons for this result were a delay of mixing of the plasma jet and the fuel jet and low temperature in the recirculation zone behind the step. Though a drastic improvement of mixing of the fuel jet with the main flow in the recirculation zone behind the step was demonstrated, the static temperature there was too low to incur a strong combustion reaction.

Nomenclature

d	=	diameter
M	=	Mach number
m	=	mass flow rate
P_{in}	=	electric power input
p_{t0}	=	total pressure
p_w	=	wall pressure
T	=	temperature
T_{t0}	=	total temperature
x, y, z	=	space coordinates
x_i	=	position of fuel injector
x_0	=	start point of the rearward-facing step
Y_j	=	mass fraction
$\Delta p_{w,\mathrm{ave}}$	=	average wall-pressure increase
δ_{in}	=	boundary-layer thickness of inflow
ω_x	=	vorticity

I. Introduction

A DUAL-MODE ramjet engine has been developed in many countries for a propulsion system in hypersonic vehicles. Reliable ignition and flame stabilization in the scramjet mode are important technologies for the success of the engine. A plasma jet (PJ) torch [1–9] has been extensively investigated as a suitable igniter in the scramjet mode. Advantages of the PJ torch are its role as a source of radicals and its higher temperature than a combustion jet. It is well known that the addition of radicals drastically reduces the ignition delay time of a combustible mixture [7]. However, quenching of the radicals via recombination reactions and a decrease in temperature of the PJ plume rapidly occur in the low-temperature main airflow. Strong combustion and flame spread in a wide area after local ignition occurs only when a fuel directly collides with the high-temperature region of the PJ core [8]. The PJ plays the role of the flame holder in the flow in the case of fuel injection upstream of the PJ. The phenomena of ignition by the PJ injected downstream of the fuel jet include both features of ignition and of flame propagation. On the other hand, it is difficult to achieve strong combustion for the case of the fuel injection downstream of the PJ [8]. As previously mentioned, one reason for this disadvantage of downstream fuel injection is the rapid decay of temperature and radical concentration in the PJ plume. The other reason is the absence of a flame-holding mechanism in the flowfield. If some flame-holding mechanism is installed, fuel injection downstream of the PJ becomes promising, because the progress of diffusion of the PJ can supply many radicals into a larger volume around the ignition site than is possible with upstream fuel injection. In the case of the upstream fuel injection, ignition occurs locally at very limited region around the PJ core.

As for achievement of flame stabilization in a supersonic flow, installation of a rearward-facing step [10–12] has been conducted by many researchers. Formation of a recirculation zone behind the step drastically increases the residence time of the fuel. Actually, the combination of a PJ torch and a rearward-facing step has been employed as an ignition system in engine tests of a subscale scramjet [13–15], in which the downstream fuel injection behind the step was adopted. However, there has been no report on the effect of a rearward-facing step on plasma ignition in a supersonic flowfield. In the present study, therefore, the authors first investigated the effect of a rearward-facing step on the ignitability of the PJ torch by a comparison with ignition tests in a straight duct. To elucidate the effect of the rearward-facing step on ignition by the PJ, three-dimensional computational fluid dynamics (CFD) analysis including a H_2/O_2 detailed chemical kinetics was also conducted.

II. Experimental Setup

A. Wind Tunnel and Test Section

The experiment was conducted using an intermittent-suction-type wind tunnel. Figure 1 shows a schematic of the test section. Atmospheric air was inhaled and accelerated to supersonic speed through a two-dimensional contoured nozzle. The test section of the straight duct without the rearward-facing step had a 30 mm square uniform cross section and was 320 mm long. The Mach number and the characteristic length for unity Reynolds number of the main flow at the PJ torch were 1.7 and $8.9 \times 10^6\ \mathrm{m}^{-1}$, respectively. The stagnation temperature and stagnation pressure were at room conditions. The origin of the Cartesian coordinate system (x, y, z) was taken at the center of the PJ torch nozzle. Streamwise, transverse, and spanwise directions correspond to x, y, and z. Success of ignition by the PJ was evaluated based on the wall pressure measured by a

Received 10 June 2008; revision received 19 December 2008; accepted for publication 5 February 2009.

*Graduate Student, Department of Aerospace Engineering.
†Associate Professor, Department of Aerospace Engineering. Member AIAA.

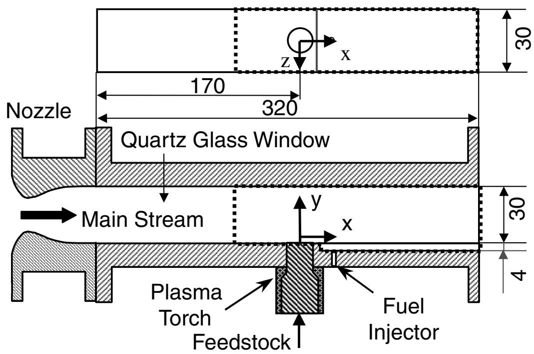

Fig. 1 Schematic of test section and computational domain.

strain-gauge-type pressure transducer. Pressure taps were installed at 10 mm intervals from upstream of the PJ to downstream of the fuel injector. The signal from the transducer was amplified by a dc amplifier and was recorded by a data recorder. The error of the pressure measurement system was estimated as less than 1.5 kPa.

A rearward-facing step was installed in the straight duct between the PJ igniter and the fuel injector, as shown in Fig. 1. The step starts at $x_0 = 14$ mm and the step height is set at 4 mm. It has been reported in [16] that this combination of the location of the fuel injector and the step height in Fig. 1 resulted in merging of the recirculation zones behind of the step surface and in front of the fuel jet. The formation of a large recirculation zone considerably increases the residence time of the fuel.

B. Plasma Torch

The same plasma torch as that used in a series of previous studies [7,8] was employed. The detailed structure has been reported in the cited papers. The cathode was made of hafnium to attain high durability when oxygen was used as the feedstock. The anode and the nozzle were made of O_2-free copper. The PJ was perpendicularly injected into the main stream at $x = 0$ mm. The diameter of the nozzle throat was 1.5 mm. O_2, N_2, and N_2/O_2 mixtures were used as feedstock gas and their mole flow rates were set the same at 1.1×10^{-2} mol/s. The error of the flow meter was less than 1.0%.

C. Fuel Injector

Three kinds of fuels (H_2, CH_4, and C_2H_4) at room temperature were tested. The fuel was perpendicularly injected into the main stream at the speed of sound from an orifice located at $x_i = 24$ mm on the centerline of the bottom wall. The diameters of the orifice were 1.0 and 1.8 mm for the straight duct and for the duct with the step, respectively. The different orifice size for the duct with the step was determined to maximize enlargement effect of recirculation zone [14] with a requirement of the same fuel equivalence ratio for both experiments with and without the rearward-facing step. The bulk equivalence ratio was set at 0.060 for all fuels and both ducts with and without the step. The ratios of the amount of heat release via complete combustion of H_2 and C_2H_4 to those of CH_4 were 1.22 and 1.11, respectively. The dynamic pressure ratios of the fuel jet and the main flow were adjusted to embody the same equivalence ratio for the all fuels. They were 4.0 for the straight duct and 1.3 for the duct with the step for H_2, 2.7 for the straight duct and 0.84 for the duct with the step for CH_4, and 1.6 for the straight duct and 0.48 for the duct with the step for C_2H_4.

III. Numerical Method

A. Governing Equations and Numerical Schemes

To clarify the detailed structure of the flowfield with the rearward-facing step, three-dimensional numerical analysis with chemical kinetics was conducted. The governing equations were the Reynolds-averaged three-dimensional Navier–Stokes equations with the k-ω shear-stress-transport two-equation turbulence model [17] and nine-species (H_2, O_2, H_2O, O, H, OH, HO_2, H_2O_2, and N_2) conservation equations in the generalized curvilinear coordinate. The convective fluxes were evaluated by the SHUS scheme [18] with the third-order MUSCL approach [19]. The viscous fluxes were evaluated by the second-order central-difference scheme. A modified LU-SGS implicit method [20] was used for temporal integration. The turbulent thermal conductivity and turbulent mass diffusivities were related to the turbulent viscosity through the specified values of the turbulent Prandtl number and the turbulent Schmidt number. In this study, they were assumed to be 0.9 and 0.5, respectively. The H_2/O_2 combustion model including 33 elementary reactions by Stahl and Walnatz [21] was used as a kinetic model.

B. Boundary Conditions and Injection Conditions of Two Jets

The computational domain is the region framed by dotted lines in Fig. 1. Calculations were conducted for the region between 50 mm upstream of the PJ torch and the exit of the test section with a length of 200 mm. The numbers of grid points were $157 \times 55 \times 71$ for the flowfield without the rearward-facing step and $175 \times 77 \times 71$ for the flowfield with the step. The smallest grid size was 20 μm near the wall. No-slip and 290 K isothermal wall conditions were assumed at the wall. The exit boundary was modeled as supersonic extrapolation. To match the realistic conditions of the experiments, the inflow conditions at the left boundary in the domain were obtained from the result of calculation for the upstream part of the test section with a length of 120 mm, the inflow Mach number of which was 1.9 at $T_{t0} = 290$ K, $p_{t0} = 0.1$ MPa, and $\delta_{\text{in}} = 2$ mm. The Mach number in the duct gradually decreased due to friction on the wall and it reached to 1.7 at the same PJ torch location as in the experiment. Hydrogen fuel was perpendicularly injected to the main stream at its sonic speed. The injection conditions and the injector position of the fuel were the same as those in the experiment.

The injection conditions of the PJ were calculated by assuming the uniform thermochemical equilibrium condition. In this simulation, oxygen was selected as the feedstock gas and the flow rate was the same as that in the experiment. The case of $P_{\text{in}} = 1.7$ kW was calculated as one typical condition. The input electric power was converted to the total enthalpy increase of feedstock gas with a specific conversion efficiency. The conversion efficiency was assumed to be 80% for oxygen feedstock based on the measurement by Sakuranaka et al. [22]. The static temperature, the static pressure, and the mole fraction of the O radical at injection were 2957 K, 157.8 kPa, and 0.075, respectively.

C. Validation of Numerical Results

The wall-pressure data obtained by computation were compared with the experiment for validation of the numerical results. The combination of H_2 fuel and O_2 PJ with relatively low-electric-power input was selected as one example. Figures 2a and 2b show comparisons of the wall-pressure distribution for the flowfield with the rearward-facing step between the experiment and the CFD. Figure 2a is the result of the upper wall and Fig. 2b is the result of the lower wall. The rearward-facing step starts at $x_0 = 14$ mm in Fig. 2. The numerical results show good agreement with experimental data. Oscillations of the wall pressure upstream of the step in the experiment were the result of reflection of weak shock waves formed at the small discontinuity between inner surfaces of the nozzle and the test section, which was not included in CFD analysis.

IV. Results and Discussion

A. Ignition Tests with and Without a Rearward-Facing Step

Wall pressure is considered to be proportional to the degree of heat release due to combustion of the fuel in a supersonic airflow. Therefore, establishment of ignition and strength of combustion were examined in relation to the wall-pressure increase. The following nondimensional averaged value of the wall-pressure increase throughout the downstream region of the PJ ($x > 0$ mm) was investigated as the parameter. The local wall-pressure increase was estimated by subtracting the wall pressure ($p_{w,\text{PJ}}$) when only the PJ was injected from that ($p_{w,\text{PJ+fuel}}$) when the PJ and the fuel jet were injected:

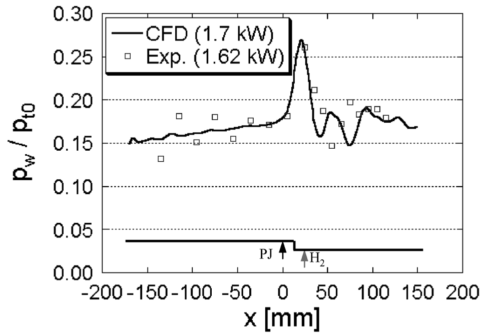

a) Upper wall

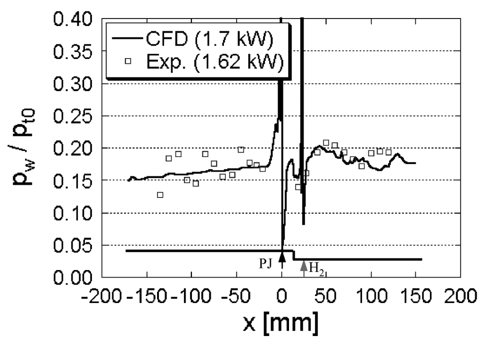

b) Lower wall

Fig. 2 Comparison of wall-pressure distribution between experiment and simulation (fuel: H_2 and PJ: O_2).

$$\Delta p_{w,\mathrm{ave}} = (p_{w,\mathrm{PJ+fuel}} - p_{w,\mathrm{PJ}})_{\mathrm{average}} / p_{t0} \qquad (1)$$

To clarify the effect of the installation of the rearward-facing step, ignition tests in the straight duct and in the duct with the rearward-facing step were conducted for three fuels. The fuels were injected at $x_i = 24$ mm, and O_2, N_2 and N_2/O_2 mixtures were used as the feedstock of the PJ torch.

Throughout the experiments with and without the rearward-facing step, unsteady phenomena such as strong oscillations of wall pressure or of the location of the pseudo shock wave (PSW) [23] were not observed. This result guaranteed the validity of using the Reynolds-averaged Navier–Stokes model in the numerical analysis.

The wall-pressure increase was not observed for the CH_4 fuel, even when the rearward-facing step was installed and the electric power input was large. This result was caused by a longer ignition delay of the CH_4 fuel than those of the H_2 and C_2H_4 fuels. Ignition of the CH_4 fuel was not achieved within the test section. In the case of fuel injection downstream of the PJ, results obtained purely reflected ignition characteristics of each fuel [24]. It can be concluded that a selection of the CH_4 as a fuel for the scramjet combustor is not realistic, though the CH_4 is considered to be one strong candidate in hydrocarbon fuels [4,7–9,25].

Figure 3 shows a comparison of the averaged wall-pressure increases due to combustion of H_2 fuel at different electric power inputs for both cases with and without the rearward-facing step. Basically, the wall-pressure increase due to combustion in the flowfield with the rearward-facing step was smaller than that in the straight duct at the same electric power input, though the fuel equivalence ratios were the same for both cases. It is noted that the threshold value of the electric power input above which strong combustion occurred and at which a large pressure increase appeared was clearly shown in the result for the duct with the rearward-facing step. The threshold P_{in} is about 2.4 kW in Fig. 3. This tendency was in contrast to the result for the straight duct, in which the wall-pressure increase was in proportion to the electric power input.

Figure 4 shows the wall-pressure increase due to combustion of C_2H_4 fuel for the flowfield with and without the rearward-facing step. Though the amount of combustion was smaller than that of the H_2 fuel, the same tendency as the result for the H_2 fuel was seen in the

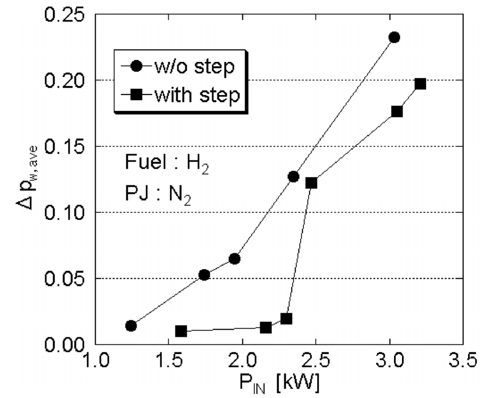

Fig. 3 Effect of the rearward-facing step on the averaged wall-pressure increase due to combustion (fuel: H_2 and PJ: N_2).

result for the C_2H_4 fuel. A jump of the wall-pressure increase for the duct with the step was observed around $P_{\mathrm{in}} = 3.0$ kW.

The wall-pressure distribution along the x axis was investigated to elucidate the reason for the behavior of the averaged wall pressure of the flowfield, with the rearward-facing step being different from that in the flowfield of the straight duct that appeared in Figs. 3 and 4. Figures 5 and 6 show wall-pressure distributions along the x axis for the cases with and without the rearward-facing step, respectively, when H_2 was injected downstream of the $N_2(50\%)/O_2(50\%)$ PJ. The data of the main flow were obtained when the PJ torch was turned off.

There was very little dependence of the wall-pressure behavior on the feedstock gas. This result indicates that the effects of NO_x, which had a catalytic effect on ignition reactions of H_2 and hydrocarbon fuels under special conditions [24,26] and was long-lived in the PJ plume [24], were not dominant for the ignition process in the experiment in this study. The amount of combustion in the flowfield of the straight duct strongly depended on the electric power input. This dependence on electric power input reflects the importance of the thermal effect of the PJ.

Figure 5 shows that the starting point of the pressure increase and the maximum wall pressure were in proportion to the electric power input in the straight duct. The behavior of the averaged wall pressure in Fig. 3 can be explained by these results. A PSW was formed when there was large electric power input in the straight duct. Figure 7 shows a typical schlieren photograph of the PSW established in the straight duct. The electric power input to the $N_2(50\%)/O_2(50\%)$ PJ was 2.99 kW. The existence of the PSW considerably enhanced the mixing and resulted in strong combustion. In Fig. 5, the PSW reached the entrance of the test section at $P_{\mathrm{in}} = 3.15$ kW and the flow became a subsonic flow. Therefore, the location of the PSW strongly affected the wall-pressure increase.

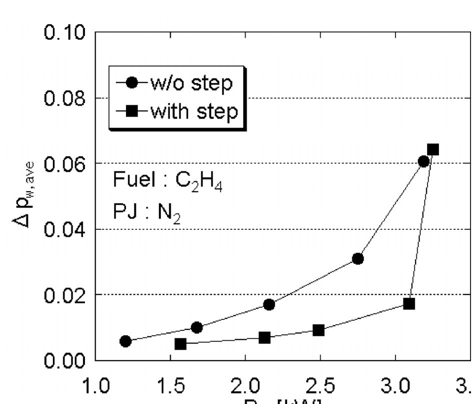

Fig. 4 Effect of the rearward-facing step on the averaged wall-pressure increase due to combustion (fuel: C_2H_4, PJ: N_2).

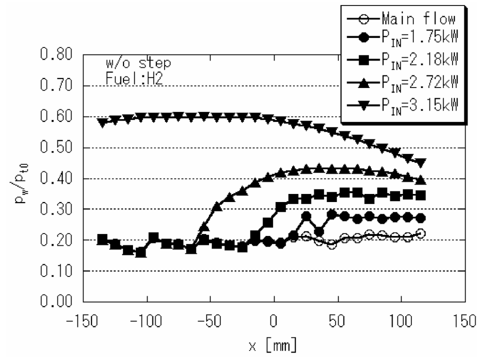

Fig. 5 Wall-pressure distributions of the flowfield without a rearward-facing step [fuel: H_2 and PJ: $N_2(50\%)/O_2(50\%)$].

On the other hand, as shown in Fig. 6, the wall pressure due to combustion was not seen in the range of low-electric-power input in the flowfield with the rearward-facing step. The reason for this low reactivity for the flowfield with the step was considered to be the low temperature and low pressure of the main flow after it passed the expansion fans at the step. The existence of expansion fans radiating from the step was also confirmed in the numerical simulation. At the large electric power input, the wall pressure increased due to combustion, as in the case of the flowfield without the step. The drastic change in the wall-pressure distribution between $P_{in} = 2.39$ and 3.08 kW corresponds to the jump of the averaged wall pressure in Fig. 4. The PSW was also formed in the flowfield with the step at large electric power input; however, the PSW did not travel further upstream beyond the step. The starting point of the wall-pressure increase did not change for the electric power input larger than 3.0 kW. The existence of the rearward-facing step kept the PSW at the step for a wide range of the electric power input.

Figure 8 show direct photographs of the PJ and the C_2H_4 flame in the flowfield with the rearward-facing step. In the combination of the N_2 PJ and a hydrocarbon fuel, a strong emission from a cyan (CN) species was detected [8]. Though the emission from the CN species was not necessarily related to the heat-release area, it was a type of index for a flame region. The strong emission around the fuel jet behind the step is clearly shown in Fig. 8; therefore, the local reaction superficially occurred at the collision area of the PJ and the fuel jet, irrespective of the existence of the rearward-facing step, but the flame area did not spread into the recirculation zone behind the step. The mechanism that enhances flame spreading after local ignition at the collision point of the PJ with the fuel jet is required to attain strong combustion around the step.

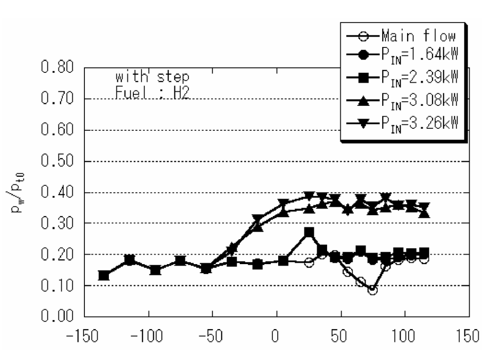

Fig. 6 Wall-pressure distributions of the flowfield with a rearward-facing step [fuel: H_2, PJ: $N_2(50\%)/O_2(50\%)$].

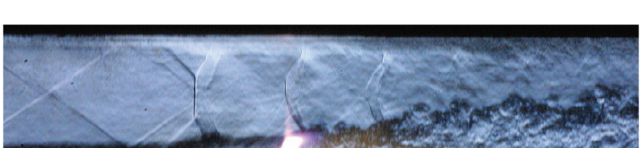

Fig. 7 Schlieren photograph of PSW established in a straight duct [fuel: H_2, PJ: $N_2(50\%)/O_2(50\%)$, and $P_{in} = 2.99$ kW].

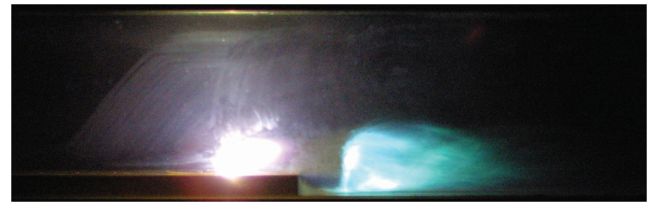

Fig. 8 Direct photographs of N_2 PJ and C_2H_4 flame in the flowfield with a rearward-facing step ($P_{in} = 2.95$ kW).

B. Numerical Results

To analyze the results of ignition tests by the PJ, three-dimensional CFD analysis with chemical kinetics was conducted. The combination of the O_2 PJ and the H_2 fuel was selected as a typical case. It was confirmed in the experiments that there was little dependence of ignition behavior on the feedstock gas to the PJ.

Figures 9a and 9b show a typical streamline of the main flow beyond the step corner and those of the PJ injected upstream of the step and the fuel jet injected downstream of the step, respectively. Various studies [10–12] on the effect of the rearward-facing step in supersonic flow have shown that a large two-dimensional recirculation zone in the x–y plane is formed between the step and the fuel jet in the flowfield without upstream PJ injection. In the present study, when the PJ was injected upstream of the step, however, the shape of such a recirculation zone changed and the recirculation zone in x–y plane disappeared around the centerline. There was a strong secondary circulation zone with low velocity toward the side wall (z direction) behind the step, as shown in Fig. 9a. The PJ collided with the upper part of the fuel jet after acceleration and declination to the lower wall by passing the expansion fans at the step. The mixing of the PJ and the fuel jet progressed downstream by the interaction of each streamwise vortices; finally, the PJ combined with the fuel jet further downstream, as shown in Fig. 9b.

Figures 10a and 10b show distributions of local equivalence ratios of the H_2 fuel for both cases with and without the rearward-facing step. The fuel jet widely diffused to the span direction behind the step. The strong secondary flows, as shown in Fig. 9a, enhanced the mixing of the fuel jet and the main airflow, and the fuel even reached the side wall. On the other hand, diffusion of the fuel to the span direction was not observed in the flowfield without the step. However, the core region in which temperature and the H_2 mass

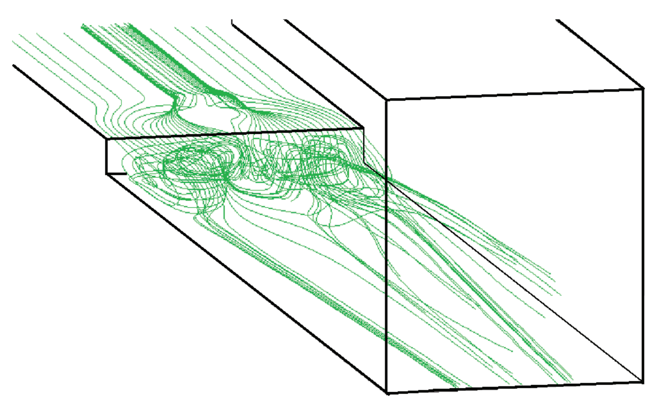

a) Main flow

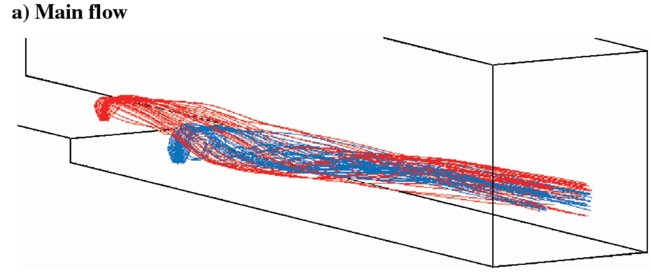

b) PJ and fuel jet

Fig. 9 Streamlines after passing the rearward-facing step in numerical simulation.

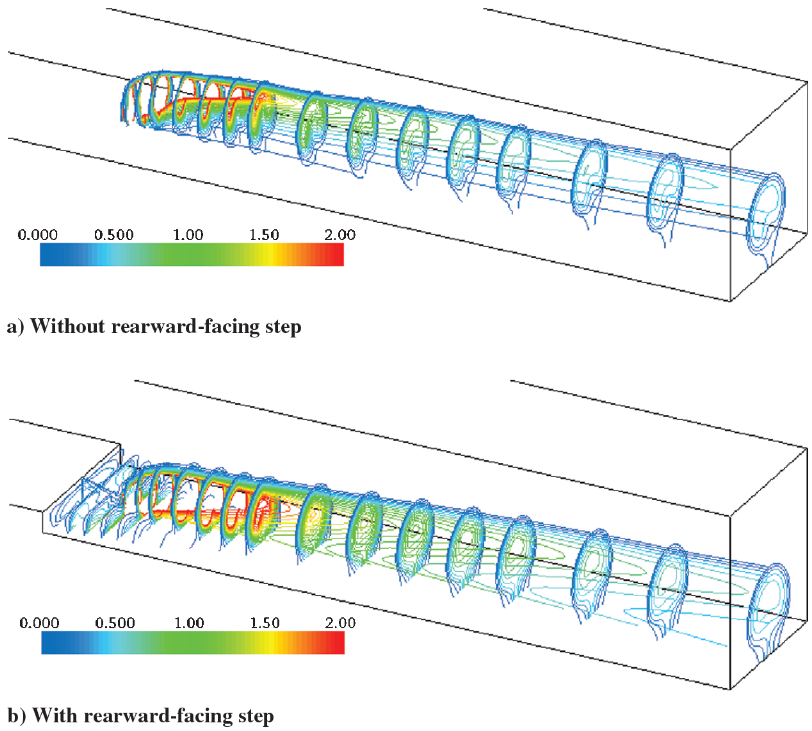

Fig. 10 Distributions of local equivalence ratio of fuel in the flowfield (fuel: H_2, PJ: O_2, P_{in} = 1.7 kW): a) without a rearward-facing step and b) with a rearward-facing step.

fraction were very high more quickly disappeared in the flowfield without the step than that in the flowfield with the step. This result indicates that the mixing of the PJ and the fuel jet was suppressed by the installation of the rearward-facing step. The difference in the mixing level was clear near the lower wall.

The detailed vortex structure of the two jets was investigated to understand the preceding result. Figures 11a and 11b show distributions of velocity vectors and vorticity in the y–z plane ($x = 28$ mm), 4 mm downstream of the location of fuel injection ($x_i = 24$ mm). In the flowfield without the step, two streamwise vortices of the PJ and of the fuel jet merged into one large vortex pair. On the other hand, the two vortices were clearly separated at the location of the fuel injection in the flowfield with the step. This decoupling of two vortices was considered to be the reason for the slow mixing of the PJ and the fuel jet in the region downstream of the fuel-injection site.

The amount of combustion and the region in which reactions occurred were compared between two flowfields with and without the rearward-facing step. Figures 12a and 12b shows distributions of H_2O mass fraction in the two cases with the same contour level. The H_2O was formed around the fuel jet and at the inside of that in the straight duct. On the other hand, the region in which reaction occurred was initially formed at only the upper part of the fuel jet and it gradually extended around the fuel jet in the flowfield with the step. A small amount of the H_2O was formed behind the step, though diffusion of the H_2 fuel was considerably progressed there, as shown in Fig. 10b. The reaction level in the straight duct was clearly higher than that in the flowfield with the step. This result agreed well with the tendency of the experiment. Decreases in pressure and temperature of the main flow after passing the expansion fans at the step and suppression of mixing between the two jets were considered to be the reasons for the low reactivity.

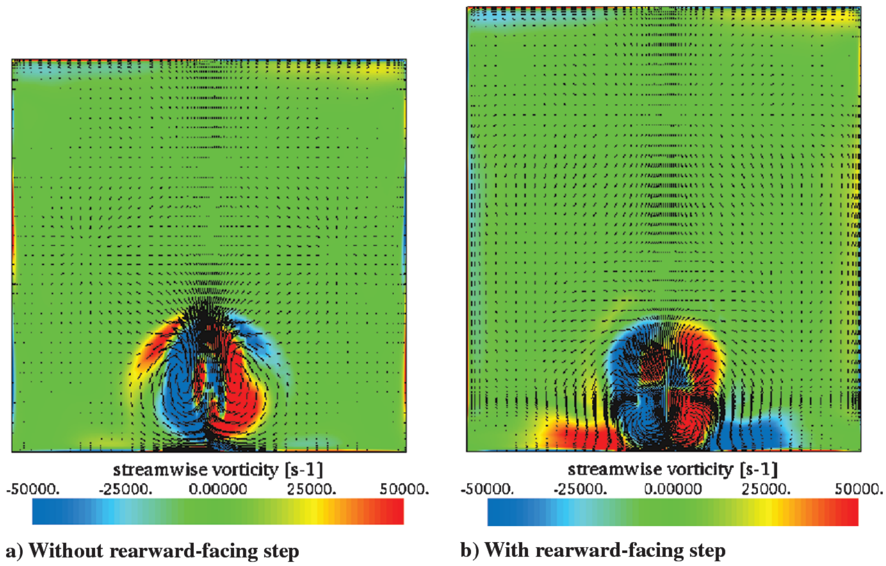

Fig. 11 Distributions of velocity vectors and vorticity in the y–z plane downstream of the fuel-injection site ($x = 28$ mm).

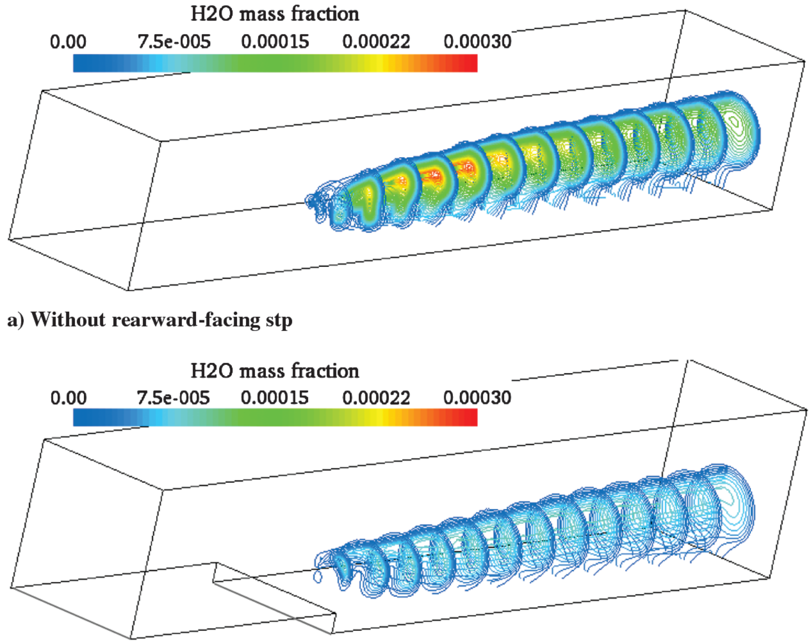

a) Without rearward-facing stp

b) With rearward-facing stp

Fig. 12 Distributions of mass fraction of H_2O in the flowfield (fuel: H_2, PJ: O_2, and $P_{in} = 1.7$ kW).

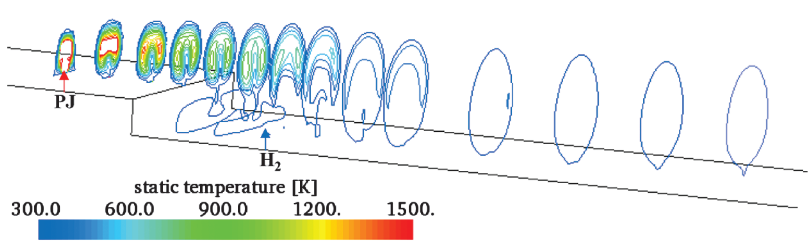

Fig. 13 Distribution of static temperature in the flowfield with a rearward-facing step (fuel: H_2, PJ: O_2, and $P_{in} = 1.7$ kW).

Figure 13 shows a distribution of static temperature in the flowfield with the step. The high temperature of the PJ core region quickly decayed, and therefore temperature considerably decreased when the mixing of the PJ and the fuel jet progressed downstream. In addition, the temperature in the recirculation zone behind the step was about 300 K. This low temperature was the reason that combustion reaction did not occur behind the step, in spite of the existence of a large amount of the fuel there. After all, a very slight effect of the installation of the rearward-facing step on enhancement of ignition and combustion was caused by slow mixing of the fuel jet and the PJ and low temperature in the recirculation zone behind the step. In addition to mixing enhancement of the fuel, diffusion enhancement of enthalpy of high-temperature PJ is required in the flowfield with low static temperature.

The low temperature in the step region was one reason for little enhancement effect of the step in this study. The total temperature in the experiments was room temperature, and therefore the experimental condition was considered to be the most severe case for ignition test. Total temperatures in the actual engine condition [27,28] or experimental conditions of the subscale-model scramjet engine tests [13–15] were much higher than those in this study. In such conditions, strong progress in mixing of the fuel jet in the recirculation zone by installation of the rearward-facing step, shown in numerical results, must contribute ignition and combustion enhancement in a supersonic flow.

V. Conclusions

This study experimentally and numerically investigated the role of the rearward-facing step for plasma ignition in a supersonic flow. Results of ignition tests showed that the installation of the rearward-facing step had an inhibition effect against the movement of the PSW beyond the step. However, the installation of the step did not show ignition and combustion enhancement effects. It was clearly shown by numerical simulation with chemical kinetics that the reasons for very slight effect of the rearward-facing step on plasma ignition were slow mixing of the PJ and the fuel jet after passing the step and low temperature in the recirculation zone behind the step. Though a drastic improvement of mixing of the fuel jet with the main flow by secondary flow toward the side wall in the recirculation zone behind the step was demonstrated, temperature in the recirculation zone was too low to incur a strong combustion reaction. In the flowfield with low static temperature, a mechanism for increase in temperature is required in addition to mixing enhancement of a fuel.

Acknowledgments

This study was supported by the Industrial Technology Research Grant Program in 2006 from New Energy and Industrial Technology Development Organization (NEDO) of Japan. The authors are grateful to Goro Masuya, Tohoku University, for his valuable comments and to Hiroyuki Mizushima for his assistance in numerical simulation. Numerical simulation was conducted by SX-9 of the Information Synergy Center at Tohoku University.

References

[1] Kimura, I., Aoki, H., and Kato, M., "The Use of a Plasma Jet for Flame Stabilization and Promotion of Combustion in Supersonic Airflows," *Combustion and Flame*, Vol. 42, No. 1981, pp. 297–305. doi:10.1016/0010-2180(81)90164-4

[2] Northam, G. B., McClinton, C. R., Wagner, T. C., and O'Brien, W. F., "Development and Evaluation of a Plasma Jet Flameholder for

Scramjets,"AIAA Paper 84-1408, 1984.

[3] Sato, Y., Sayama, M., Ohwaki, K., Masuya, G., Komuro, T., Kudou, K., Murakami, A., Tani, K., Wakamatsu, Y., Kanda, T., Chinzei, N., and Kimura, I., "Effectiveness of Plasma Torches for Ignition and Flameholding in Scramjet," *Journal of Propulsion and Power*, Vol. 8, No. 4, 1992, pp. 883–889.
doi:10.2514/3.23565

[4] Shuzenji, K., and Tachibana, T., "Superiority of Oxygen as Feedstock for a Plasma Jet Igniter in Supersonic Methane Air Streams," *Proceedings of the Combustion Institute*, Vol. 29, No. 1, 2002, pp. 875–881.
doi:10.1016/S1540-7489(02)80112-2

[5] Jacobsen, L. S., Gallimore, S. D., O'Brien, W. F., and Schetz, J. A., "Integration of an Aeroramp Injector/Plasma-Igniter for Hydrocarbon Scramjets," *Journal of Propulsion and Power*, Vol. 19, No. 2, 2003, pp. 170–182.
doi:10.2514/2.6114

[6] Gallimore, S. D., Jacobsen, L. S., O'Brien, W. F., and Schetz, J. A., "Operational Sensitivities of an Integrated Scramjet Ignition/Fuel-Injection System," *Journal of Propulsion and Power*, Vol. 19, No. 2, 2003, pp. 183–189.
doi:10.2514/2.6116

[7] Takita, K., Moriwaki, A., Kitagawa, T., and Masuya, G., "Ignition of H_2 and CH_4 in High Temperature Airflow by Plasma Torch," *Combustion and Flame*, Vol. 132, No. 4, 2003, pp. 679–689.
doi:10.1016/S0010-2180(02)00518-7

[8] Kitagawa, T., Moriwaki, A., Murakami, K., Takita, K., and Masuya, G., "Ignition Characteristics of Methane and Hydrogen Using a Plasma Torch in Supersonic Flow," *Journal of Propulsion and Power*, Vol. 19, No. 5, 2003, pp. 853–858.
doi:10.2514/2.6175

[9] Shuzenji, K., and Tachibana, T., "Advantage of Using Oxygen as Plasma Jet Feedstock for Methane/Air Ignition," *Journal of Propulsion and Power*, Vol. 21, No. 5, 2005, pp. 908–913.
doi:10.2514/1.8668

[10] Uenishi, K., Rogers, R. C., and Northam, G. B., "Numerical Predictions of a Rearward-Facing-Step Flow in a Supersonic Combustor," *Journal of Propulsion and Power*, Vol. 5, No. 2, 1989, pp. 158–164.
doi:10.2514/3.23131

[11] Abbitt, J. D., Segal, C., McDaniel, J. C., Krauss, R. H., and Whitehurst, R. B., "Experimental Supersonic Hydrogen Combustion Employing Staged Injection Behind a Rearward-Facing Step," *Journal of Propulsion and Power*, Vol. 9, No. 3, 1993, pp. 472–478.
doi:10.2514/3.23646

[12] Karagozian, A. R., Wang, K. C., Le, A. T., and Smith, O. I., "Transverse Gas Jet Injection Behind a Rearward-Facing Step," *Journal of Propulsion and Power*, Vol. 12, No. 6, 1996, pp. 1129–1136.
doi:10.2514/3.24153

[13] Masuya, G., Kudou, K., Murakami, A., Komuro, T., Tani, K., Kanda, T., Wakamatsu, Y., Chinzei, N., Sayama, M., Ohwaki, K., and Kimura, I., "Some Governing Parameters of Plasma Torch Igniter/Flame-holder in a Scramjet Combustor," *Journal of Propulsion and Power*, Vol. 9, No. 2, 1993, pp. 176–181.
doi:10.2514/3.23606

[14] Kanda, T., Saito, T., Kudo, K., Komuro, T., Ono, F., and Matsui, A., "Mach 6 Testing of a Scramjet Engine Model," *Journal of Propulsion and Power*, Vol. 13, No. 4, 1997, pp. 543–551.
doi:10.2514/2.5201

[15] Kobayashi, K., Tomioka, S., and Mitani, T., "Supersonic Flow Ignition by Plasma Torch and H_2/O_2 Torch," *Journal of Propulsion and Power*, Vol. 20, No. 2, 2004, pp. 294–301.
doi:10.2514/1.1760

[16] Zamma, Y., Shiba, H., Masuya, G., Tomioka, S., Hiraiwa, T., and Mitani, T., "Similarity parameters of Pre-Ignition Flowfields in a Supersonic Combustor," AIAA Paper 97-2890, 1997.

[17] Menter, F. R., "Two-Equation Eddy-Viscosity Turbulence Models for Engineering Applications," *AIAA Journal*, Vol. 32, No. 8, 1994, pp. 1598–1605.
doi:10.2514/3.12149

[18] Shima, E., and Jounouchi, T., "Role of CFD in Aeronautical Engineering—AUSM Type Upwind Schemes," *Proceedings of the 14th NAL Symposium on Aircraft Computational Aerodynamics*, NAL-SP-34, National Aerospace Labs., Chofu, Japan, 1994, pp. 255–260.

[19] Ju, Y., "Lower-Upper Scheme for Chemically Reacting Flow with Finite Rate Chemistry," *AIAA Journal*, Vol. 33, No. 8, 1995, pp. 1418–1425.
doi:10.2514/3.12564

[20] Yoon, S., and Jameson, A., "Lower-Upper Symmetric-Gauss-Seidel Method for the Euler and Navier–Stokes Equations," *AIAA Journal*, Vol. 26, No. 9, 1988, pp. 1025–1026.
doi:10.2514/3.10007

[21] Stahl, G., and Walnatz, J., "Numerical Investigation of Time-Dependent Properties and Extinction of Strained Methane- and Propane-Air Flamelets," *Combustion and Flame*, Vol. 85, Nos. 3–4, 1991, pp. 285–299.
doi:10.1016/0010-2180(91)90134-W

[22] Sakuranaka, N., Mitani, T., Izumikawa, M., Sayama, M., and Ohwaki, K., "Thermal Efficiency of Plasma Torch Igniter," *Proceedings of the Thirty-Third Space Science and Technology Conference*, 1989, pp. 56–57 (in Japanese).

[23] Masuya, G., Choi, B., Ichikawa, N., and Takita, K., "Mixing and Combustion of Fuel Jet in Pseudo-Shock Waves," AIAA Paper 2002-0809, 2002.

[24] Takita, K., Abe, N., Masuya, G., and Ju, Y., "Ignition Enhancement by Addition of NO and NO_2 from a N_2/O_2 Plasma Torch in a Supersonic Flow," *Proceedings of the Combustion Institute*, Vol. 31, No. 2, 2007, pp. 2489–2496.
doi:10.1016/j.proci.2006.07.108

[25] Lewis, M. J., "Significance of Fuel Selection for Hypersonic Vehicle Range," *Journal of Propulsion and Power*, Vol. 17, No. 6, 2001, pp. 1214–1221.
doi:10.2514/2.5866

[26] Han, B., Sung, C. J., and Nishioka, M., "Effects of Vitiated Air on Hydrogen Ignition in a High-Speed Laminar Mixing Layer," *Combustion Science and Technology*, Vol. 176, No. 3, 2004, pp. 305–330.
doi:10.1080/00102200490256018

[27] Mitani, T., "Ignition Problems in Scramjet Testing," *Combustion and Flame*, Vol. 101, No. 3, 1995, pp. 347–359.
doi:10.1016/0010-2180(94)00218-H

[28] Bonanos, A. M., Schetz, J. A., O'Brien, W. F., and Goyne, C. P., "Dual-Mode Combustion Experiments with an Integrated Aeroramp-Injector/Plasma-Torch Igniter," *Journal of Propulsion and Power*, Vol. 24, No. 2, 2008, pp. 267–273.
doi:10.2514/1.28301

I. Boyd
Associate Editor